Available online at www.sciencedirect.com

ScienceDirect

journal homepage: www.elsevier.com/locate/issn/15375110

Research Paper

Multi-temporal imaging using an unmanned aerial vehicle for monitoring a sunflower crop

Francisco Agüera Vega [a,b,c,*], *Fernando Carvajal Ramírez* [a,b], *Mónica Pérez Saiz* [a,b], *Francisco Orgaz Rosúa* [b,d]

[a] *Departamento de Ingeniería, Universidad de Almería, Almería, Spain*
[b] *Campus de Excelencia Internacional Agroalimentaria ceiA3, Spain*
[c] *Campus Universitario, Escuela Superior de Ingeniería, 04120, Almería, Spain*
[d] *Departamento de Producción Vegetal, Instituto de Agricultura Sostenible, Córdoba, Spain*

ARTICLE INFO

Article history:
Received 24 October 2014
Received in revised form
11 January 2015
Accepted 31 January 2015
Published online 18 February 2015

Keywords:
Unmanned aerial vehicle image
Sunflower
Multispectral sensor
NDVI

The objective of this study is to determine the capability of an unmanned aerial vehicle system carrying a multispectral sensor to acquire multitemporal images during the growing season of a sunflower crop. Measurements were made at different times of the day and with different resolutions to estimate the normalised difference vegetation index (NDVI) and study its relationship with several indices related to crop status with the aim of generating useful information for application to precision agriculture techniques. NDVI was calculated from images acquired on four different dates during the cropping season. On two of these dates, two images were acquired to determine how the time of day when the images were taken influences NDVI value. To study the influence of image resolution on NDVI, the original images were resampled to 30 × 30 and 100 × 100 cm pixel sizes. The results showed that the linear regressions between NDVI and grain yield, aerial biomass and nitrogen content in the biomass were significant at the 99% confidence level, except during very early growth stages, whereas the time of day when the images were acquired, the classification process, and image resolution had no effect on the results. The methodology provides information that is related to crop yield from the very early stages of growth and its spatial variability within the crop field to be harvested, which can subsequently be used to prescribe the most appropriate management strategy on a site-specific basis.

1. Introduction

Precision agriculture (PA) is a production method that takes into account the spatial variability of conditions that affect crop production (e.g., soil characteristics, land elevation and weed infestation) and uses the information related to this variability to determine the most effective management strategy (Brisco, Brown, Hirose, Mcnairn, & Staenz, 1998; Moran, Inoue, & Barnes, 1997). The main steps of PA are data collection, field-variability mapping, decision-making, and

* *Corresponding author*. Departamento de Ingeniería, Universidad de Almería, Almería, Spain. Fax: +34 950215491.
E-mail address: faguera@ual.es (F.A. Vega).
http://dx.doi.org/10.1016/j.biosystemseng.2015.01.008
1537-5110/

the application of the management practices (Zhang and Kovacs, 2012). Remote sensing techniques can be used in the first three steps of the workflow (Copenhaver, 1998; Lan, Thomson, Huang, Hoffmann, & Zhang, 2010; Stafford, 1999; Warren & Metternicht, 2005), especially when the field variability maps are elaborated or updated to aid farmers to adapt the appropriate strategy that is based on variable management practices within a field according to the site conditions. The information needed to apply PA is provided by new technologies, such as geographic information systems (GIS), global positioning system (GPS), remote sensing, yield monitoring devices, and machinery that is able to apply the inputs in a variable-rate manner (Seelan, Laguette, Casady, & Seielstad, 2003). Gathering the required information is one of the key issues in PA that needs to be addressed to design appropriate decision systems and to recognise significant temporal variations (Lan et al. 2010; McBratney, Whelan, & Shatar, 1997).

To gather information for PA, several sensor platforms, including satellites and aircraft, have been used. Nevertheless, the platforms are not wholly adequate to provide information at the required spatial and time resolutions, as the images taken from them are expensive, and they can be affected by weather conditions such as clouds (Ehsani, Sankaran, Maja, & Camargo Neto, 2014; Hunt et al., 2014). Even the latest generation of very high resolution satellite images (e.g., GeoEye-1 and WorldView-2) is not able to provide high frequency data for critical situations such as monitoring nutrients or water stresses, diseases, or pest attacks. Moreover, manned airborne platforms are limited because of their high operational complexity, cost and the long time needed to deliver the images (Rango et al. 2009).

Unmanned aerial vehicles (UAV) have undergone a remarkable development in recent years and are now powerful sensor-bearing platforms for various agricultural and environmental applications. A limited amount of research on UAV applications for PA has been published. For example, Hunt, Cavigelli, Daughtry, McMurtrey, and Walthall (2005) used an unmanned helicopter with an image acquisition system to estimate biomass and nitrogen status for corn, alfalfa, and soybeans crops. Berni, Zarco-Tejada, Suarez, and Fereres (2009) acquired thermal and narrow band multispectral images taken from an unmanned helicopter to estimate biophysical parameters that were strongly correlated with leaf area index, chlorophyll content and water stress. Swain, Thomson, and Jayasuriya (2010) used a radio-controlled unmanned helicopter platform to acquire quality spatial and temporal resolution images to estimate grain yield and total aerial biomass of a rice crop. Linear regressions between these parameters and the normalised difference vegetation index (NDVI; Rouse, Hass, Schell, & Deering, 1973), estimated from images, yielded significant regression coefficients of 0.728 and 0.760, respectively. Agüera, Carvajal, and Saiz (2011) found a good correlation between applied nitrogen and NDVI that was estimated from images acquired from a quadrocopter flying at 70 m altitude over a sunflower crop.

Baluja et al. (2012) employed a UAV equipped with a multispectral sensor and a thermal camera to assess the water status of a commercial rain-fed vineyard of Tempranillo cv. (*Vitis vinifera* L.). Zarco-Tejada, Gonzalez-Dugo, and Berni (2012) demonstrated the ability to track stress levels in a citrus crop using thermal and hyperspectral imagery acquired from a UAV. García-Ruiz et al. (2013) used a UAV equipped with a multispectral camera to identify a citrus greening disease affecting citrus orchards. Recently, Hutn et al. (2014) used a sensor mounted on a UAV to collect imagery of a potato crop in near-infrared (NIR), red and green bands. From these images, they calculated the NDVI and green normalized difference vegetation index (GNDVI) and their relationship with leaf area index, plant cover and chlorophyll content over the growing season.

Because UAVs fly at low altitudes, ultra-high spatial resolution images can be obtained at a low operational cost, and the images can be acquired as frequently as necessary and analysed in quasi-real-time (Agüera et al. 2011; Hardin & Hardin, 2010; Xiang & Tian, 2011). Thus, it is necessary to study the application of images from UAVs for PA.

The objective of the present study is to determine the capability of a system composed of a UAV carrying a multispectral sensor (red, green and near infrared bands) to acquire multitemporal images during the growth season of a sunflower crop at different times of the day and with different resolutions to estimate the normalized difference vegetation index (NDVI) and study its relationship with several indices related to crop status with the aim of generating useful information that can be applied to precision agriculture.

2. Materials and methods

2.1. *Field experiment*

The experiment was conducted at the Agricultural Research Centre of Córdoba (37°51′22″ N, 4°48′19″ W), southern Spain. The soil is a deep sandy-loam, classified as Typic Xerofluvent (Driessen & Dudal, 1991). Córdoba has a Mediterranean-type climate with high temperatures in the summer, and most of the rainfall is concentrated between the autumn and spring.

A PR64E71 sunflower (*Helianthus annuus*, L.) hybrid crop was sown on 23 February 2012 with a plant density of 7.1 plants m^{-2}, which is a plant population widely used by local farmers.

The field was 30 × 30 m (Fig. 1), and two perpendicular strips divided the field into four blocks, each with a different irrigation treatment: full irrigation, which covered 100% of the crop's water need (I1); full irrigation until anthesis and no irrigation afterwards (I2), which simulated a typical sunflower season in this area; half irrigation (I3), which covered 50% of the crop's water needs; and no irrigation (I4). The irrigation treatment began on 25 May 2012. Each of these four blocks was divided into eight elemental plots of 7 × 3.4 m^2 (11 rows with 17 plants each), corresponding to eight nitrogen treatments, and which resulted in 32 elemental plots. The nitrogen application rates were 0, 20, 40, 60, 80, 100, 120 and 140 kg [N] ha^{-1}; half was applied on the sowing date, and the second half was applied on 20 May 2012. The experimental design was not intended to study the influence of irrigation or nitrogen application on crop yield. Rather, the objective was to simulate a high variability of growing conditions to study the relation of NDVI with several indices related to crop status. A

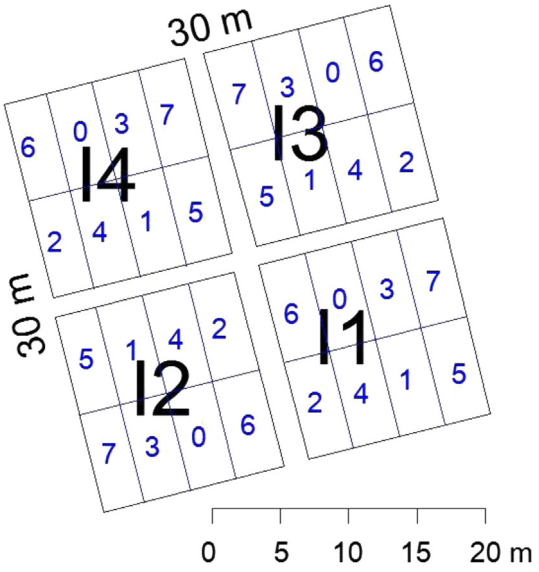

Fig. 1 – Plot layout of the experimental field. I1, I2, I3 and I4 correspond to full irrigation, full irrigation until anthesis and no irrigation after anthesis, 50% of water needs irrigation, and no-irrigation treatment, respectively. Numbers 0 to 7 represent the nitrogen application rate: 0, 20, 40, 60, 80, 100, 120 and 140 kg [N] ha^{-1}, respectively.

similar experimental design has been used in other works. For example, Tremblay, Vigneault, Bélec, Fallon, and Bouroubi (2014) who designed an experiment with eight unreplicated N treatment rates, two sowing dates, two fields (one loamy and one clayey) and with or without irrigation, for comparing the performance of UAV and satellite imagery (Pléiades-1B) for nitrogen status assessment in a corn crop.

At the end of the season, interference from birds made it impossible to harvest the crop of 13 of the elemental plots. The sole possible effect on the data is a reduction in the range of environmental conditions, but considering that the number of nitrogen doses was very high and that the affected elemental plots were randomly distributed over the whole plot, there was a sufficient range of growth conditions over the remaining 19 elemental plots to ensure the generality of the results.

On 10 July, at the physiological maturity stage, the five central rows of the 19 elemental plots were hand harvested, and the seven central plants of each row were taken. This avoided harvesting plants that were close to another elemental plot that had a different nitrogen treatment. Yield (kg ha^{-1}), aboveground biomass (kg ha^{-1}) and nitrogen content in the biomass (g [N] kg^{-1}) were estimated for each of the elemental plots. To estimate the yield, the grain was manually separated from the rest of the plant. Aboveground biomass was determined by drying the harvested plants at 60 °C until a constant mass was attained. The nitrogen content in the biomass was measured with an automated nitrogen analyser.

2.2. *Unmanned aerial platform and digital camera*

A Tetracam ADC Lite digital camera (TETRACAM INC., Chatsworth, CA, USA), was mounted on a Microdrones MD4-200 (Microdrones GmbH's VTOL UAV, Siegen, Germany), to take images of the field experiment during the crop season. The Tetracam ADC Lite is a single CMOS camera with a resolution of 1200 × 1024 pixels. Images were acquired in raw format. Colour reconstruction of the raw images (de-mosaicing processing using raw pixel data) was carried out using PixelWrech2 (TETRACAM INC., Chatsworth, CA, USA), which is a multispectral imaging editing software package included with the Tetracam camera. After colour reconstruction, the green, red and near infrared (G, R, NIR) spectral bands approximately covered the following wavelength intervals: 520–570 nm (G), 600–690 nm (R) and 750–850 nm (NIR). Hunt et al. (2014) found that a source of error in this process is the colour correction matrix that is included in the Tetracam PixelWrench software because the best matrix cannot be determined if the spectral response function of the camera sensor is not known. These researchers concluded that sensor calibration is important when comparing data acquired on different dates or from different locations. In our case, the data were collected using a single picture, and all of the data were related to crop yield components.

The Microdrones MD4-200 can be programmed to follow a route defined by several way-points and actions. With a flight altitude of 75 m, in combination with the camera focal length, only one picture was necessary to cover the entire experimental field.

Several tasks were necessary to make the camera fully operational: a camera mount and an electrical power circuit were built, and a servomechanism to control the shutter of the camera was installed. The Tetracam ADC Lite digital camera mounted on the Microdrones MD4-200 is shown in Fig. 2.

2.3. *Image acquisition*

Images were acquired on four different dates during the crop season: 27 April 2012 (phenological stage: V6, (Schneiter & Miller, 1981)), 19 May 2012 (phenological stage: R1), 30 May 2012 (phonological stage: R3) and 23 June 2012 (phenological stage: R5, full anthesis). All of the images were acquired at midday, except on 30 May, when due to technical problems the image was acquired at 20:00 h under sunset light conditions. Furthermore, on 19 May and 23 June a second image was taken at 16:30 h. Hence, a total of six images were taken over

Fig. 2 – The Microdrones MD4-200 UAV with Tetracam ADC Lite that was used for image acquisition.

the season. Figure 3 shows the developmental stages of the sunflower crop at the dates when the images were acquired.

At the beginning of the season, several targets were placed on the ground in the corners of the plots. To georeference the images, the coordinates of four targets were measured with a Trimble R6 GPS receiver. On 27 April, a picture was taken with an RGB digital camera (Fig. 4) and georeferenced using the ground control points. From the georeferenced image, the coordinates of the corners of the elemental plots were deduced. The four targets of the corners of the main experimental field were maintained throughout the crop season, so that the pictures taken with the Tetracam could be georeferenced and the elemental plots could be identified in the images.

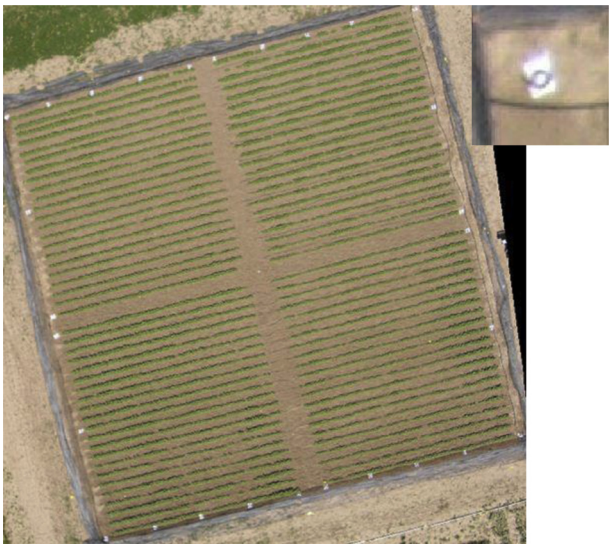

Fig. 4 – Field experiment RGB image with targets for elemental plot identification and georeferencing. In the upper right corner, a detailed enlargement of a target image is shown.

2.4. *Image processing*

After the colour reconstruction of the raw images using the PixelWrench2 software (http://www.tetracamera.com/Products_PixelWrench2.htm, last visit October 2014), a set of TIFF images was produced.

The Ortho-Engine module in the PCI V10.0 software (http://www.pcigeomatics.com/software/geomatica/education, last visit October 2014) was used to georeference the images using the targets mentioned in Section 2.3 as ground control points. Thus, at the end of this process, a set of six georeferenced images of the experimental field was acquired over the crop season. Based on the sensor characteristics and the camera height, the ground resolution cell was 1 × 1 cm. Furthermore, each image was resampled to a ground resolution cell of 30 × 30 cm and 100 × 100 cm, to study the influence of image resolution on the estimated NDVI value. Therefore, with the initial resolution of 1 × 1 cm, a set of 18 images was used in this study. The nearest neighbour interpolation method was used to resample the images, which identified the grey level of the pixel closest to the specified input coordinates and assigned that value to the output coordinates (Lopes, Touzi, & Nezry, 1990). NDVI was estimated as follows (Eq. (1)):

$$\mathrm{NDVI} = (\mathrm{NIR} - \mathrm{red})/(\mathrm{NIR} + \mathrm{red}), \quad (1)$$

where red and NIR are the digital values of the pixels corresponding to those bands.

In an effort to avoid the influence of soil and shadow on the NDVI estimation, a previous image classification process was

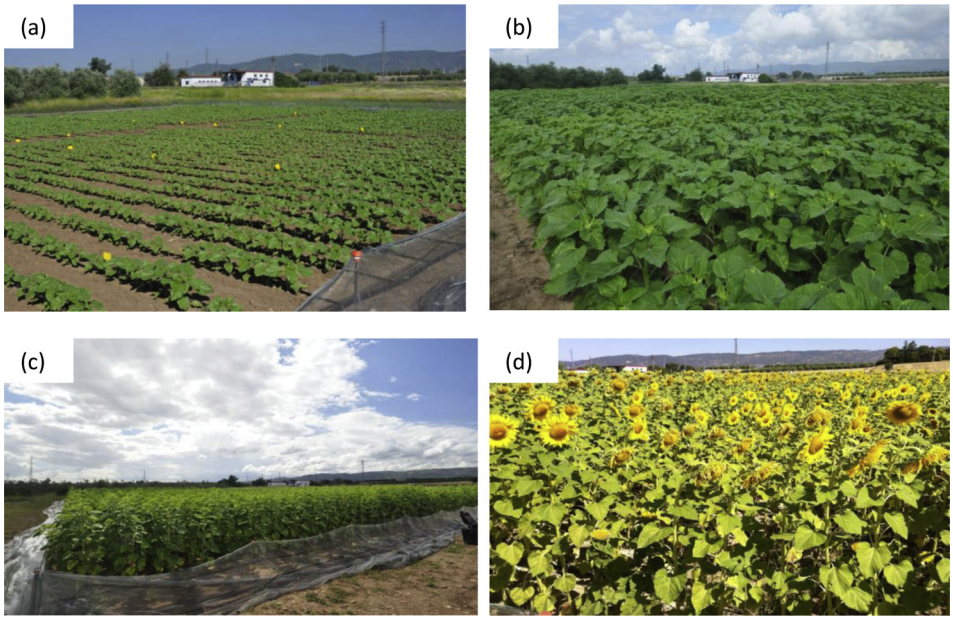

Fig. 3 – The sunflower crop when the images were taken on 27 April 2012 (a), 19 May 2012 (b), 30 May 2012(c) and 23 June 2012 (d).

conducted with the goal of detecting the crop. This process was only performed on the 1 × 1 cm and 30 × 30 cm pixel resolution images because it was not possible to distinguish the crop, bare soil and shadows in the 100 × 100 cm resolution images. Maximum likelihood classification (MLC), which is a classifier that only takes into account the land-use spectral signatures, was used for the supervised image classification. Only the crop class was taken into account, but as a means of improving the classification process, the class was divided into three sub-classes according to tonality (light, medium and dark). The result of the process was a set of binary images for which the presence (crop) and absence (no crop) of crops was discerned.

Next, the digital numbers of each band for each elemental plot of each image were extracted. This was done using a Visual Basic 6.0 computer program developed by the authors. The program inputs were the classification results and the coordinates of the corner of each elemental plot. The program reads the coordinates of the image pixels and the digital number corresponding to each band. From the classification results, it checked whether the pixel was classified as crop and, if so, determined the elemental plot that contained the pixel. Then, a file for each elemental plot was generated and the digital number that corresponded to each band of each pixel classified as crop was written into the file. For the unclassified images (100 × 100 cm resolution), the digital numbers were directly extracted, regardless of the classification results. The NDVI of each elemental plot and each image was estimated from those data.

3. Results and discussion

3.1. *Images classification*

Figure 5a shows the six false-colour images with 1 × 1 cm of pixel resolution acquired over the season, and Fig. 5b shows the original images taken on 19 May at midday with 1 × 1 cm of pixel resolution and the resampled images with 30 × 30 and 100 × 100 cm resolutions.

The classification process used to detect the crop gave good results for all analysed images, with an overall classification accuracy over 85% in all cases. Figure 6 shows the 1 × 1 cm pixel resolution image classification for 27 March; the areas that are classified as sunflower are red and the remaining land cover is black. The results agree with those of other authors working with the same image classification method to detect crops. Thus, the overall classification accuracy achieved by Kun, Bingfang, Yichen, Yuan, and Qiangzi (2011) to distinguish different crops was greater than 95%. Lu, Oki, Shimizu, and Omasa (2007) reported classification accuracies from 79.5 to 100% when detecting plant species near metropolitan Tokyo, Japan.

3.2. *Relation of NDVI and yield, aerial biomass and nitrogen content in the biomass*

Tables 1–3 show the correlation coefficients for the fitted linear models that describe the relationships between NDVI and grain yield, aerial biomass and nitrogen content in the biomass, respectively, for all of the cases.

As seen in the three tables, data covering a phenological range from R1 (mid-May) to R5 (end-June) showed similar values and were statistically significant at the 99% confidence level. The exceptions were data corresponding to the first date (first row of Tables 1–3). This non-significant relationship at the beginning of the season was expected because the crop had not yet shown differences due to the nitrogen or irrigation treatments. Working with sunflower, Peña-Barragan, Lopez-Granados, Jurado-Exposito, and Garcia-Torres (2010) found a coefficient correlation value of 0.6 for the linear model between the yield and NDVI calculated at the R1 phenological stage (early reproductive phase), which is similar to those shown in the second and third rows of Table 1. Meanwhile, Reyniers and Vrindts (2006) found correlation coefficients of 0.53, 0.63 and 0.48, corresponding to the linear regressions between NDVI calculated from an Ikonos satellite image that was acquired at the end of the growing season of a wheat crop and the grain yield, aerial biomass, and nitrogen content in the biomass, respectively.

With respect to image resolution and image classification, the data did not reflect any differences. Thus, the accuracy of the linear regression between the yield and NDVI was the same when images with 1 × 1, 30 × 30, or 100 × 100 cm of pixel resolution were compared.

The same result occurred when the effect of image classification was studied: no differences were found between the correlation coefficients of the linear regressions for the classified images and those fitted for the unclassified images. Thus, the elimination of bare soil using the image classification process had no effect on the calculation of NDVI. In agreement with those results, Myneni and Williams (1994) found a good relationship between NDVI and canopy vigour and colour, even in the presence of pixel heterogeneity. Flowers, Weisz, Heiniger, Tarleton, and Meijer (2003) reported similar results using infrared photography when studying the in-season nitrogen status in winter wheat. Tremblay et al. (2014), who were working with a maize crop and multispectral imagery acquired from an UAV, observed that image segmentation did not practically improve the correlation coefficient between the soil-adjusted vegetation index (SAVI) and fresh biomass or leaf area index. In a sunflower crop, Peña-Barragan et al. (2010) found that the best correlation coefficients between NDVI calculated from an aerial image and harvest indexes were associated with images that were acquired around maximum vegetative development or during early productive development. To explain these results, they theorized that the images acquired outside these stages had pixels that were composed of a mixture of vegetation and bare soil. Zarco-Tejada, Ustin, and Whiting (2005) reported that the best relationships were obtained in the early cotton growth stages using structural indexes such as NDVI and concluded that those indexes were better indicators of yield variability during early growth stages. Similar results were reported by Yang, Bradford, and Wiegand (2001) for yield estimation of cotton, grain sorghum and maize crops. Their results indicated that images acquired around maximum vegetative development or during early productive development best described yield variability. This trend was not observed in the

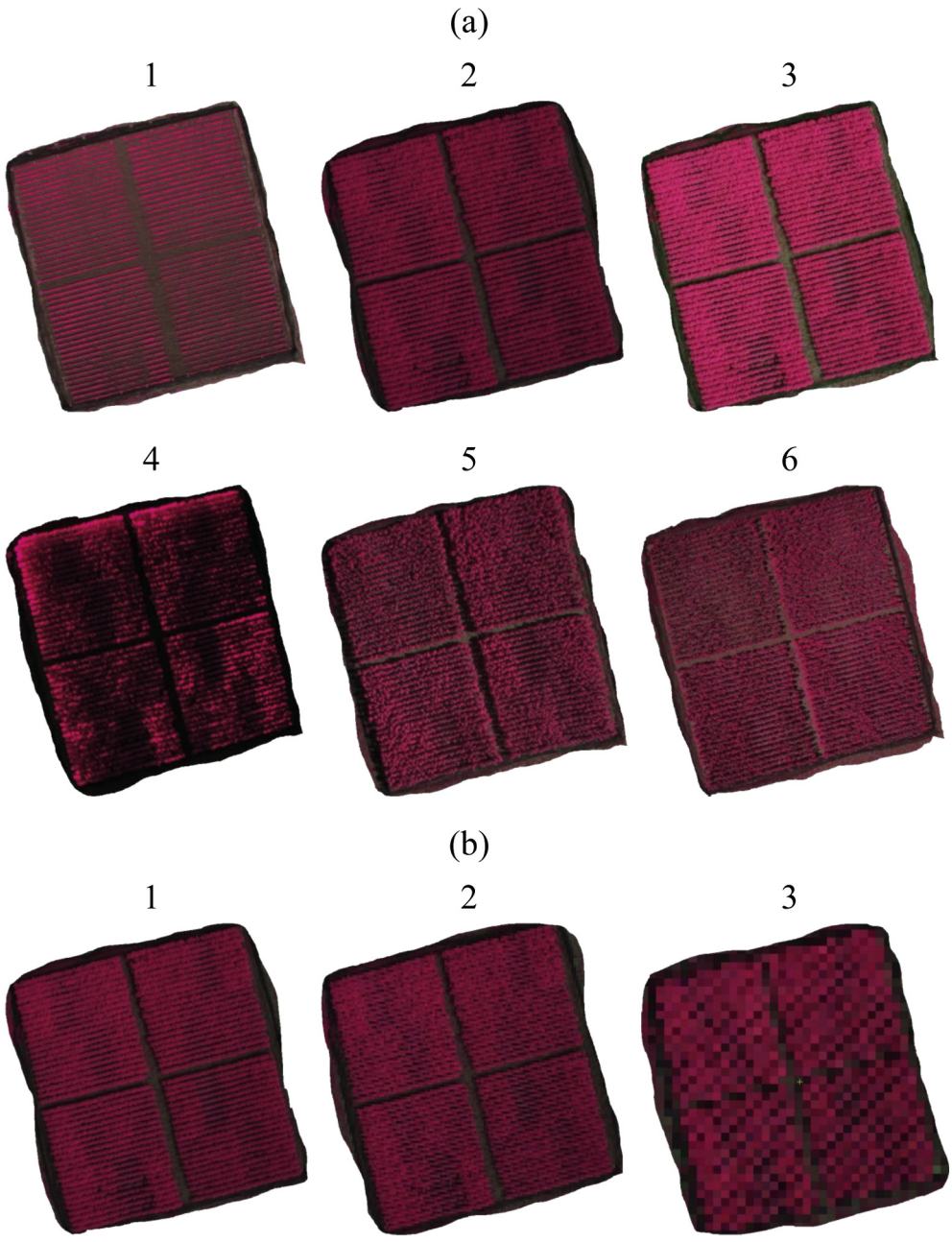

Fig. 5 – (a) False colour images with 1 cm^2 pixel resolution: 1) 27 March 2011 midday, 2) 19 May 2011 midday, 3) 19 May 2011 afternoon, 4) 30 May 2011 afternoon, 5) 23 June 2011 midday, 6) 23 June 2011 afternoon. (b) Image acquired on 19 May midday, at 1) 1 × 1 cm pixel resolution, 2) 30 × 30 cm pixel resolution and 3) 100 × 100 m pixel resolution.

data shown in Tables 1–3; the correlation coefficients were similar for all dates except for the first of them, which was at a very early growing stage when the crop had not yet shown the effects of nitrogen or irrigation treatments.

Tables 1–3 show that the time of the data collection had practically no effect on the results that corresponded to images taken on the same date. Even the image acquired at 20:00 h under extreme light conditions yielded statistically significant correlation coefficients. Furthermore, all of the linear relationships between NDVI calculated from the imagery acquired at midday and in the afternoon showed a statistically significant correlation coefficient and a regression coefficient equal to one. In agreement with those results, Reyniers (2003) found that while the reflectance values for red, green, blue, and NIR wavelengths changed with changing incident light intensity, the resulting NDVI varied only very slightly.

As a result, we were able to obtain a good correlation between NDVI and grain yield, aerial biomass and nitrogen content in the aerial biomass, with the NDVI indexes calculated from the R-G-NIR images acquired from the early reproductive stage (R1) to the flowering stage (R5), independent of image resolution (from 1 × 1 to 100 × 100 cm) and independent of image classification to extract the crop.

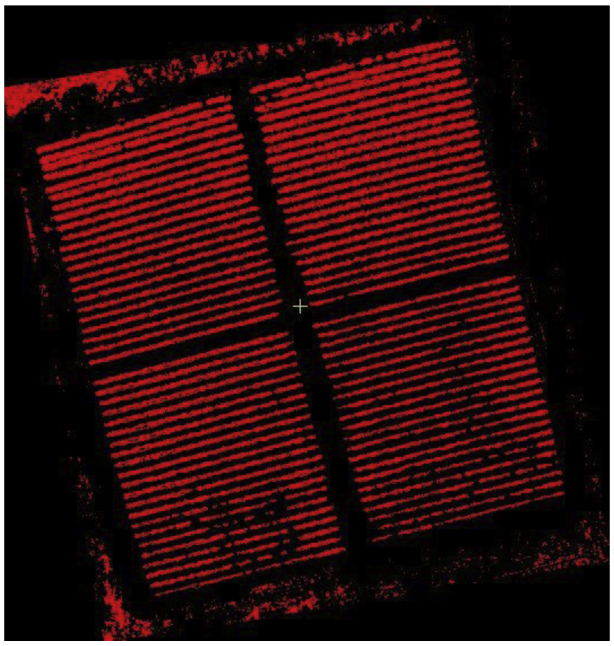

Fig. 6 – Image classification output corresponding to the Tetracam image taken on 27 March 2012. Areas in red represent land classified as sunflower, and areas in black represent the rest of the land cover.

4. Conclusions

In this study, a UAV-mounted multispectral sensor (R, G, NIR) system was used to obtain images of a sunflower crop throughout the growth season to enable NDVI to be calculated. The correlation coefficients of linear regressions fitted between NDVI and grain yield, aerial biomass and nitrogen content in the biomass were statistically significant except very early during the growing season. Thus, the NDVIs of a sunflower crop, estimated from images taken with a R, G, NIR sensor mounted on a UAV and acquired in the R1 stage, when the floral button begin to be visible, to R5 (full anthesis), can be used to detect differences in grain yield, aerial biomass and nitrogen content in the biomass within crop fields. Furthermore, images taken at an appropriate time can enable the early recognition of certain problems in the crop without waiting until harvest to detect low yield zones. This allows the farmer to apply PA techniques, adapting the dose of the treatment (e.g., irrigation, nitrogen and phytosanitary products) to the specific needs of each specific site in the crop field, with the economic, environmental and health benefits that this entails.

As the NDVIs measured were not influenced by the hour when the images were taken, images can be acquired at any time of the day, thereby eliminating the constraint of time from the task of taking images. Furthermore, image resolution caused no significant differences in the calculated regression coefficients. Thus, the flight altitude can be increase to achieve

Table 1 – Linear model correlation coefficients that describe the relationships between NDVI calculated from Tetracam images and grain yield, taking into account the date when the images were acquired, time, image resolution and if the image was classified. Except for the data corresponding to the first row, all of the data are statistically significant at the 99% confidence level.

Date	Resolution	1 × 1 cm	1 × 1 cm	30 × 30 cm	30 × 30 cm	100 × 100 cm
	Time	Classified	Not classified	Classified	Not classified	Not classified
27 March	midday	0.136	0.150	0.060	0.120	0.125
19 May	midday	0.744	0.739	0.691	0.775	0.511
19 May	afternoon	0.770	0.698	0.775	0.690	0.765
30 May	afternoon	0.736	0.816	0.708	0.818	0.739
23 June	midday	0.750	0.861	0.737	0.844	0.651
23 June	afternoon	0.834	0.673	0.625	0.719	0.715

Table 2 – Linear model correlation coefficients that describe the relationships between NDVI calculated from Tetracam images and aerial biomass, taking into account the date when the images were acquired, time, image resolution and if the image was classified. Except for the data corresponding to the first row, all of the data are statistically significant at the 99% confidence level.

Date	Resolution	1 × 1 cm	1 × 1 cm	30 × 30 cm	30 × 30 cm	100 × 100 cm
	Time	Classified	Not classified	Classified	Not classified	Not classified
27 March	midday	0.171	0.145	0.048	0.136	0.129
19 May	midday	0.748	0.897	0.681	0.864	0.595
19 May	afternoon	0.953	0.922	0.762	0.764	0.765
30 May	afternoon	0.684	0.820	0.557	0.737	0.607
23 June	midday	0.773	0.573	0.722	0.849	0.686
23 June	afternoon	0.398	0.420	0.565	0.672	0.745

Table 3 – Linear model correlation coefficients that describe the relationships between NDVI calculated from the Tetracam images and the nitrogen content in the aerial biomass, taking into account the date when the images were acquired, time, image resolution and if the image was classified. Except for the data corresponding to the first row, all of the data are statistically significant at the 99% confidence level.

Date	Resolution	1 × 1 cm	1 × 1 cm	30 × 30 cm	30 × 30 cm	100 × 100 cm
	Time	Classified	Not classified	Classified	Not classified	Not classified
27 March	midday	0.088	0.100	0.043	0.156	0.126
19 May	midday	0.773	0.954	0.675	0.796	0.656
19 May	afternoon	0.980	0.967	0.813	0.735	0.796
30 May	afternoon	0.800	0.897	0.838	0.863	0.823
23 June	midday	0.772	0.527	0.602	0.705	0.591
23 June	afternoon	0.445	0.478	0.549	0.447	0.446

an equivalent pixel size of 100 × 100 cm, which will reduce the number of images and the flight time for a given plot.

The classification process followed by the use of the images to detect the crop and calculate the NDVI from only pixels corresponding to crop did not improve the correlation coefficients studied.

Images can be taken at critical moments throughout the growing season with the type of platform and sensor used in this work, without the limitation that result from weather conditions or device availability. This is an advantage over satellites and aircraft, which have many more operational restrictions than UAVs such as used in this study.

The low cost of the aerial platform and sensor used in this work compared to the cost of a satellite image, the absence of limitations due to meteorological conditions (especially clouds), and the fact that the images are immediately available, make the described equipment and methodology useful for estimating certain crop indices for the application of PA techniques.

Acknowledgments

This work was supported by grant P08-TEP-3870 from CICE-Junta de Andalucía (Spain) and was co-financed with European Union FEDER funds.

REFERENCES

Agüera, F., Carvajal, F., & Saiz, M. (2011). Measuring sunflower nitrogen status from an unmanned aerial vehicle-based system and on the ground device. In *International Archives of the Photogrammetry, Remote Sensing and Spatial Information Sciences, XXXVIII-1/C22. ISPRS ICWG I/V UAV-g2011 (unmanned aerial vehicle in geomatics) conference, Zurich, Switzerland*.

Baluja, J., Diago, M. P., Balda, P., Zorer, R., Meggio, F., Morales, F., et al. (2012). Assessment of vineyard water status variability by thermal and multispectral imagery using an unmanned aerial vehicle (UAV). *Irrigation Science, 30*, 511–522.

Berni, J. A. J., Zarco-Tejada, P. J., Suarez, L., & Fereres, E. (2009). Thermal and narrowband multispectral remote sensing for vegetation monitoring from an unmanned aerial vehicle. *IEEE Transactions on Geoscience and Remote Sensing, 47*, 722–738.

Brisco, B., Brown, R. J., Hirose, T., Mcnairn, H., & Staenz, K. (1998). Precision agriculture and the role of remote sensing: a review. *Canadian Journal of Remote Sensing, 24*, 315–327.

Copenhaver, K. (1998). *Remote sensing can identify nitrogen stress while you have time to arrest yield loss. Chlorophyll cops*. Available online at http://precisionag.iftd.org.

Driessen, P. M., & Dudal, R. (1991). *The major soils of the world*. KULeuven Koninklijke Wöhrmann B. V., Zutphen, The Netherlands: Agricultural University Wageningen.

Ehsani, R., Sankaran, S., Maja, J. M., & Camargo Neto, J. (2014). Affordable multi-rotor remote sensing platform for applications in precision horticulture. In *12th International Conference on Precision Agriculture*. Sacramento: California, USA.

Flowers, M., Weisz, R., Heiniger, R., Tarleton, B., & Meijer, A. (2003). Field validation of a remote sensing technique for early nitrogen application decisions in wheat. *Agronomy Journal, 95*, 167–176.

Garcia-Ruiz, F., Sankaran, S., Maja, J. M., Lee, W. S., Rasmussen, J., & Ehsani, R. (2013). Comparison of two aerial imaging platforms for identification of Huanglongbing-infected citrus trees. *Computers and Electronics in Agriculture, 91*, 106–115.

Hardin, P. J., & Hardin, T. J. (2010). Small-scale remotely piloted vehicles in environmental research. *Geography Compass, 4*, 1297–1311.

Hunt, E. R., Cavigelli, M., Daughtry, C. S. T., McMurtrey, J. E., & Walthall, C. L. (2005). Evaluation of digital photography from model aircraft for remote sensing of crop biomass and nitrogen status. *Precision Agriculture, 6*, 359–378.

Hunt, E. R., Jr., Horneck, D. A., Hamm, P. B., Gadler, D. J., Bruce, A. E., Turner, R. W., et al. (2014). Detection of nitrogen deficiency in potatoes using small unmanned aircraft systems. In *12th International Conference on Precision Agriculture*. Sacramento: California, USA.

Kun, J., Bingfang, W., Yichen, T., Yuan, Z., & Qiangzi, L. (2011). Vegetation classification method with biochemical composition estimated from remote sensing data. *International Journal of Remote Sensing, 32*(24), 9307–9325.

Lan, Y., Thomson, S. J., Huang, Y., Hoffmann, W. C., & Zhang, H. (2010). Current status and future directions of precision aerial application for site-specific crop management in the USA. *Computers and Electronics in Agriculture, 74*, 34–38.

Lopes, A., Touzi, R., & Nezry, E. (1990). Adaptative speckle filters and scene heterogeneity. *IEEE Transaction on Geoscience and Remote Sensing, 28*(6), 992–1000.

Lu, S., Oki, K., Shimizu, Y., & Omasa, K. (2007). Comparison between several feature extraction/classification methods for mapping complicated agricultural land use patches using airborne hyperspectral data. *International Journal of Remote Sensing, 28*(5), 963–984.

McBratney, A. B., Whelan, B. M., & Shatar, T. (1997). Variability and uncertainty in spatial, temporal and spatio-temporal crop yield and related data. In *Precision agriculture: Spatial and temporal variability of environmental quality* (pp. 141–160). Chichester: Wiley.

Moran, M. S., Inoue, Y., & Barnes, E. M. (1997). Opportunities and limitations for image-based remote sensing in precision crop management. *Remote Sensing of Environment, 61*, 319–346.
Myneni, R. B., & Williams, D. L. (1994). On the relationship between FAPAR and NDVI. *Remote Sensing of Environment, 49*(3), 200–211.
Peña-Barragan, J. M., Lopez-Granados, F., Jurado-Exposito, M., & Garcia-Torres, L. (2010). Sunflower yield related to multi-temporal aerial photography, land elevation and weed infestation. *Precision Agriculture, 11*, 568–585.
Rango, A., Laliberte, A. S., Herrick, J. E., Winters, C., Havstad, K., Steele, C., et al. (2009). Unmanned aerial vehicle-based remote sensing for rangeland assessment, monitoring, and management. *Journal of Applied Remote Sensing, 3*, 033542.
Reyniers, M. (2003). *Precision farming techniques to support grain crop production*. PhD dissertation. Katholieke Universieit Leuven, Faculty of Applied Bioscience and Engineering.
Reyniers, M., & Vrindts, E. (2006). Measuring wheat nitrogen status from space and ground-based platform. *International Journal of Remote Sensing, 27*(3), 549–567.
Rouse, J. W., Hass, R. H., Schell, J. A., & Deering, D. W. (1973). Monitoring vegetation systems in the great plains with ERTS. In *Proceedings of the third ERTS symposium* (pp. 309–317). Washington: NASA. NASA special publication No. 351.
Schneiter, A. A., & Miller, J. F. (1981). Description of sunflower growth stages. *Crop Science, 21*, 901–903.
Seelan, S. K., Laguette, S., Casady, G. M., & Seielstad, G. A. (2003). Remote sensing applications for precision agriculture: a learning community approach. *Remote Sensing of Environment, 88*, 157–169.
Stafford, J. V. (1999). An investigation into the within-field spatial variability of grain quality. In J. V. Stafford (Ed.), *Precision Agriculture, Proceedings of Second European Conference on Precision Agriculture, Odense, Denmark* (pp. 353–361). Sheffield, UK: Academic Press.
Swain, K. C., Thomson, S. J., & Jayasuriya, H. P. W. (2010). Adoption of an unmanned helicopter for low-altitude remote sensing to estimate yield and total biomass of a rice crop. *Transactions of the ASABE, 53*, 21–27.
Tremblay, N., Vigneault, P., Bélec, C., Fallon, E., & Bouroubi, M. Y. (2014). A comparison of performance between UAV and satellite imagery for N status assessment in corn. In *12th International Conference on Precision Agriculture*. Sacramento: California, USA.
Warren, G., & Metternicht, G. (2005). Agricultural applications of high-resolution digital multispectral imagery: evaluating within-field spatial variability of canola (*Brassica napus*) in Western Australia. *Photogrammetric Engineering and Remote Sensing, 71*, 595–602.
Xiang, H., & Tian, L. (2011). Method for automatic georeferencing aerial remote sensing (RS) images from an unmanned aerial vehicle (UAV) platform. *Biosystems Engineering, 108*, 104–113.
Yang, C., Bradford, J. M., & Wiegand, C. L. (2001). Airborne multispectral imagery for mapping variable growing conditions and yields of cotton, grain sorghum, and corn. *Transaction of ASAE, 44*, 1983–1994.
Zarco-Tejada, P. J., Gonzalez-Dugo, V., & Berni, J. A. J. (2012). Fluorescence, temperature and narrow-band indices acquired from UAV platform for water stress detection using micro-hyperspectral imager and thermal camera. *Remote Sensing of Environment, 117*, 322–337.
Zarco-Tejada, P. J., Ustin, S. L., & Whiting, M. L. (2005). Temporal and spatial relationships between within-field yield variability in cotton and high-spatial hyperspectral remote sensing imagery. *Agronomy Journal, 97*, 641–653.
Zhang, C., & Kovacs, J. M. (2012). The application of small aerial systems for precision agriculture: a review. *Precision Agriculture, 13*, 693–712.